

1                   **Latest Results from the Daya Bay Reactor Neutrino Experiment**

2                   Wenqiang Gu on behalf of the Daya Bay Collaboration  
3                   *Shanghai Jiao Tong University, China*  
4                   *goowenq@gmail.com*

5                   Utilizing six powerful nuclear reactors as antineutrino sources, and eight functionally identical  
underground detectors for a near-far relative measurement, the Daya Bay Reactor Neutrino  
Experiment has achieved unprecedented precision in measuring the neutrino mixing angle  
 $\theta_{13}$  and the neutrino mass squared difference  $|\Delta m_{ee}^2|$ . With the largest sample of reactor  
antineutrino interactions ever collected to date, Daya Bay is also able to perform a number of  
other measurements in neutrino physics, such as a high-statistics determination of the absolute  
reactor antineutrino flux and spectrum, as well as a search for sterile neutrino mixing.

6                   **1 Introduction**

7                   Neutrino oscillation was first proposed by Bruno Pontecorvo in 1957<sup>1</sup>. In the past 20 years, it  
8                   has been confirmed and precisely measured over a broad range of neutrino sources. Neutrino  
9                   mixing can be characterized with a unitary Pontecorvo-Maki-Nakagawa-Sakata (PMNS) matrix,  
10                   $U_{\text{PMNS}}$ . In the three-flavor model,  $U_{\text{PMNS}}$  is commonly parameterized by the three mixing angles  
11                  ( $\theta_{12}$ ,  $\theta_{23}$ ,  $\theta_{13}$ ), a charge parity (CP) phase, and two mass-squared differences ( $\Delta m_{32}^2$ ,  $\Delta m_{21}^2$ ).

For reactor-based experiments, the survival probability of the electron antineutrino can be expressed using

$$P(\bar{\nu}_e \rightarrow \bar{\nu}_e) = 1 - \sin^2 2\theta_{13} \sin^2(\Delta m_{ee}^2 \frac{L}{4E}) - \sin^2 2\theta_{12} \cos^4 \theta_{13} \sin^2(\Delta m_{21}^2 \frac{L}{4E}) \quad (1)$$

12                  where  $\sin^2(\Delta m_{ee}^2 \frac{L}{4E}) \equiv \cos^2 \theta_{12} \sin^2(\Delta m_{31}^2 \frac{L}{4E}) + \sin^2 \theta_{12} \sin^2(\Delta m_{32}^2 \frac{L}{4E})$ . In 2012, Daya Bay  
13                  experiment first observed the last unknown mixing angle  $\theta_{13}$  with more than  $5\sigma$  significance<sup>2</sup>  
14                  shortly after the evidence of non-zero  $\theta_{13}$  noticed by the Double Chooz experiment<sup>3</sup>. Also, RENO  
15                  collaboration confirmed the result with a significance of  $4.9\sigma$  in the same year<sup>4</sup>. The discovery of  
16                  a non-zero  $\theta_{13}$  paved the way for determining the neutrino mass hierarchy (MH) and searching  
17                  for the CP violation in neutrino oscillation experiments. The same oscillation experiments can  
18                  also search for extra generations of neutrinos, the so-called “sterile neutrino”. In 2011, Huber  
19                  and Mueller *et al.* improved the theoretical treatment of the reactor antineutrino spectrum, and  
20                  found that the predicted antineutrino flux appeared higher than the measurements from the  
21                  previous short-baseline experiments. This is commonly referred as the “Reactor Antineutrino  
22                  Anomaly” (RAA)<sup>5</sup>. One possible solution for RAA is the existence of one or more eV-mass-  
23                  scale sterile neutrinos. Therefore, it is also of great interest to search for light sterile neutrino  
24                  in reactor-based experiments.

25                   **2 The Daya Bay Reactor Neutrino Experiment**

26                   The Daya Bay reactor neutrino experiment is built close to the Daya Bay Nuclear Power Plant  
27                  (NPP), one of most powerful nuclear reactor complex in the world (Fig. 1). The experiment

28 is designed to precisely measure  $\theta_{13}$ , benefitting from the near-far relative measurement which  
cancels most of the reactor related systematic uncertainty.

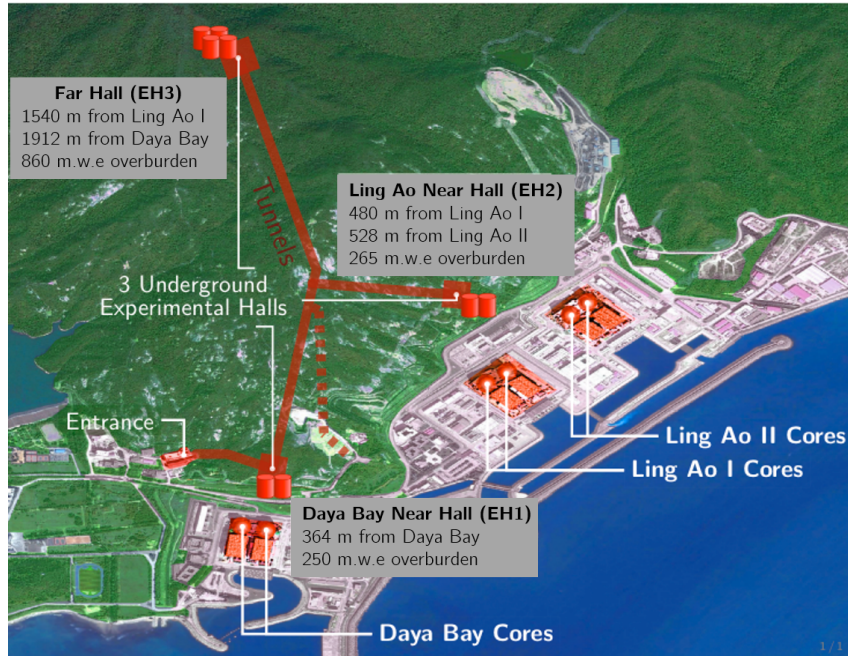


Figure 1 – Layout of the Daya Bay Reactor Neutrino Experiment.

29  
30 In each experimental hall (Fig. 2), a water Cherenkov detector and a resistive plate chamber  
31 (RPC) were built as the active muon veto. Two functionally identical antineutrino detectors  
32 (ADs) were installed in two near experimental halls, and four identical ADs were installed in  
33 the far experimental hall. The antineutrino detector had a three-zone cylindrical design, where  
34 the inner-most acrylic tank contained 20 tons of Gd-doped liquid scintillator (GdLS), and the  
35 outer acrylic vessel (OAV) was filled with 22 tons of liquid scintillator (LS), serving as the  
36 “gamma catcher” to maximize the energy detection efficiency from antineutrino interactions in  
37 the GdLS, while the region between OAV and the outer-most stainless steel (SS) tank was filled  
with mineral oil (MO) as the buffer shielding. The inverse beta decay (IBD,  $\bar{\nu}_e + p \rightarrow e^+ + n$ )

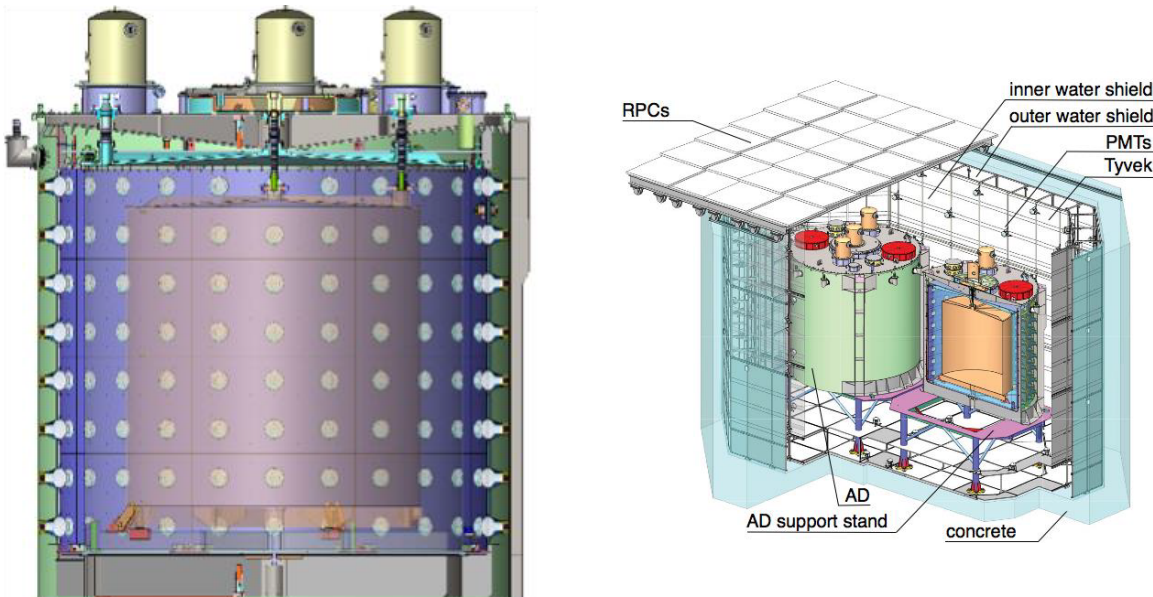


Figure 2 – Left: scheme of an antineutrino detector. Right: overview of a near experimental hall.

reaction is utilized to detect electron antineutrinos from the reactor, where a coincidence of consecutive signals are produced. The “prompt” signal arises from the kinetic energy deposition and the annihilation of the positron, while the “delayed” signal comes from the de-excitation  $\gamma$  of the neutron capture on hydrogen (2.2MeV) or gadolinium ( $\approx$ 8MeV) in the LS and GdLS. The mean lifetime for the free neutron is around  $30\mu\text{s}$  in the target.

### 3 Results

With 1230 days of data collection, Daya Bay experiment has accumulated more than 2.5 million inverse beta decay interactions, the largest sample of reactor antineutrino interactions ever collected to date.

#### 3.1 Oscillation analysis based on n-Gd sample

By selecting the IBD candidates with the neutron capture on gadolinium (n-Gd) and by performing a relative measurement on the rate deficit and energy spectrum distortion through the detectors in the near halls and in the far hall, the parameters controlling the electron antineutrino oscillation are obtained<sup>6</sup>

$$\sin^2 2\theta_{13} = 0.0841 \pm 0.0027(\text{stats.}) \pm 0.0019(\text{syst.}) \quad (2)$$

$$\Delta m_{ee}^2 = (2.50 \pm 0.06(\text{stats.}) \pm 0.06(\text{syst.})) \times 10^{-3}\text{eV}^2 \quad (3)$$

$$\Delta m_{32}^2(\text{normal}) = (2.45 \pm 0.06(\text{stats.}) \pm 0.06(\text{syst.})) \times 10^{-3}\text{eV}^2 \quad (4)$$

$$\Delta m_{32}^2(\text{inverted}) = (-2.56 \pm 0.06(\text{stats.}) \pm 0.06(\text{syst.})) \times 10^{-3}\text{eV}^2, \quad (5)$$

where  $\Delta m_{32}^2$  differs slightly for the assumption of normal mass ordering, or inverted mass ordering. Fig. 3 shows the reconstructed positron energy spectrum of the IBD candidates in the far hall. The expected spectrum assuming no oscillation, as well as the best-fit spectrum with oscillation and the background spectrum, is also overlaid. Fig. 4 shows the confidence interval

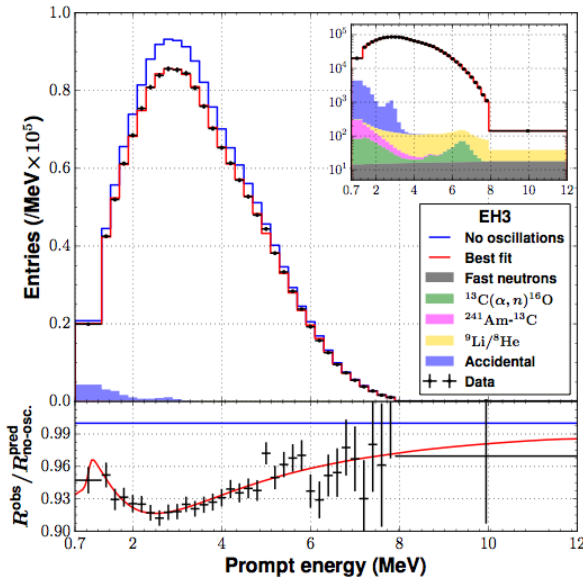


Figure 3 – Reconstructed positron energy spectrum of the antineutrino candidates in the far hall (black dots), the prediction assuming no oscillation (blue line) and the best-fit based on three-flavor neutrino model (red line). Underneath the energy spectrum is the ratio of the measured to the prediction assuming no oscillation.

for  $\Delta m_{ee}^2$  and  $\sin^2 2\theta_{13}$ , as well as the electron antineutrino survival probability as function of L/E. Almost a full cycle of  $\theta_{13}$  oscillation is covered by the data points.

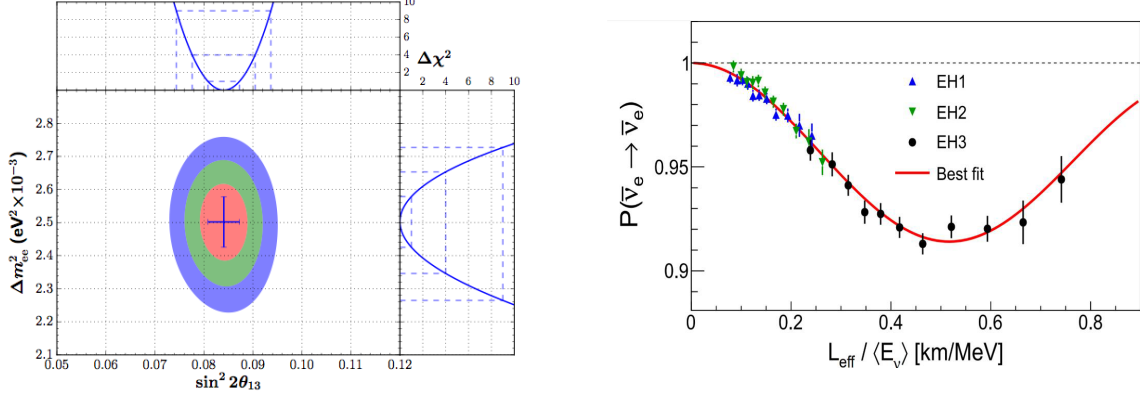


Figure 4 – Left: confidence interval for  $\Delta m^2_{ee}$  and  $\sin^2 2\theta_{13}$ . Right: the measured electron antineutrino survival probability versus  $L_{eff}/\langle E_\nu \rangle$ , where  $L_{eff}$  is the effective baseline to reactors and  $\langle E_\nu \rangle$  is the average antineutrino energy.

### 55 3.2 Oscillation analysis based on n-H sample

With 621 days of neutrino data, more than 1.2 million inverse beta decay interactions, an independent analysis based on the IBD sample with neutron capture on hydrogen (n-H) is developed <sup>7</sup>. As shown in Fig. 5, the oscillation parameter is measured to be

$$\sin^2 2\theta_{13} = 0.071 \pm 0.011 \quad (6)$$

, consistent with the Gd-capture analysis.

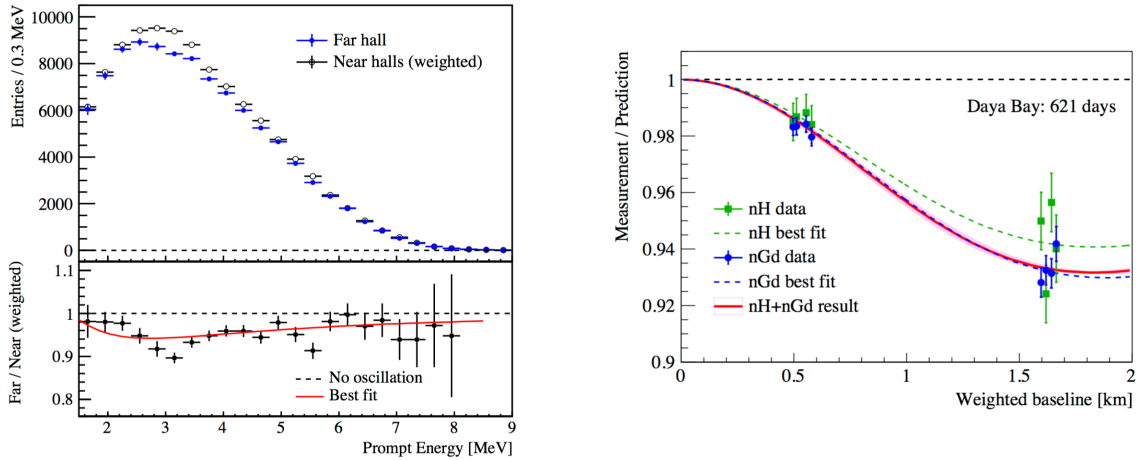


Figure 5 – Left: positron energy spectrum of the n-H IBD sample, and the best-fit of neutrino oscillation. Right: the ratio of measured candidates to the predicted candidates assuming no oscillation in each detector versus the baseline. The n-Gd sample and the best-fit are also overlaid.

56

### 57 3.3 Search for light sterile neutrino

58 A search for light sterile neutrino oscillation in the electron antineutrino disappearance channel  
 59 was carried out with the full configuration of the Daya Bay experiment <sup>8</sup>. Through a relative  
 60 comparison of the antineutrino energy spectra in the near halls and far hall, no evidence of extra  
 61 oscillation mode is found. With 621 days of data, a most stringent limits to date is achieved on  
 62  $\sin^2 2\theta_{14}$  in the  $2 \times 10^{-4} < |\Delta m^2_{41}| < 0.2 \text{ eV}^2$  region, as shown in the left panel of Fig. 6.

63 On the other hand, the constraints on  $\sin^2 2\theta_{24}$  derived from a search for muon (anti)neutrino  
 64 disappearance in the NuMI beam was performed independently by the MINOS experiment. As  
 65 shown in the right panel of Fig. 6 the combined analysis of the MINOS and the Daya Bay, as

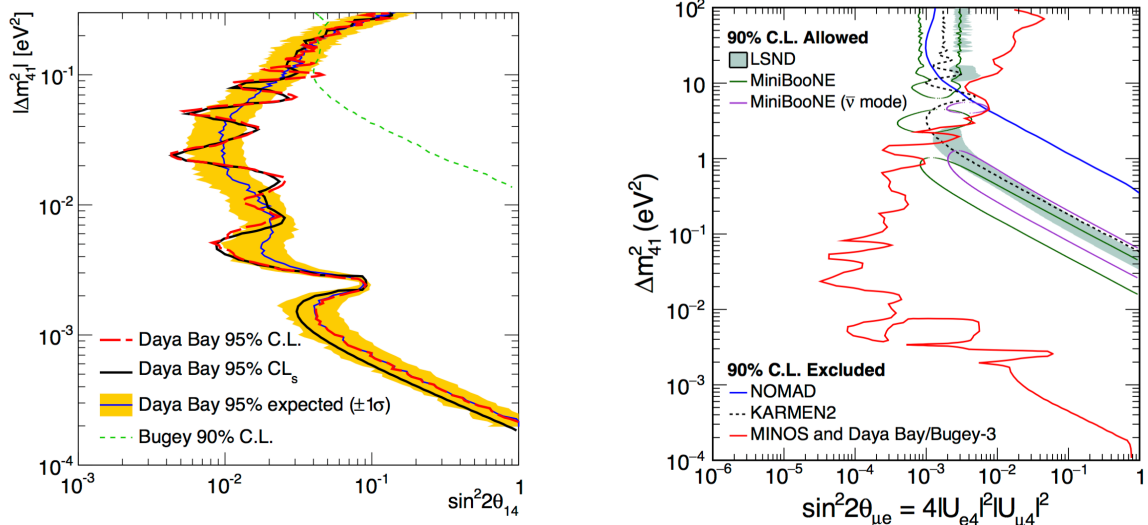


Figure 6 – Left: sterile neutrino exclusion contour in  $|\Delta m_{41}^2|$  vs.  $\sin^2 2\theta_{14}$  from Daya Bay. Right: sterile neutrino constraint in  $|\Delta m_{41}^2|$  vs.  $\sin^2 2\theta_{\mu e}$  for the  $\nu_\mu - \nu_e$  appearance channel established with a combined analysis of MINOS, Daya Bay, and Bugey-3 experiments.

well as the data from Bugey-3, provides the a very tight constraint on  $\sin^2 2\theta_{\mu e}$  over 6 orders of magnitude in  $\Delta m_{41}^2$ , based on a “3+1” picture of sterile neutrino<sup>9</sup>. The sterile neutrino mixing parameter space allowed by LSND and MiniBooNE experiments is excluded for  $\Delta m_{41}^2 < 0.8 \text{ eV}^2$  at a 95% CLs.

### 3.4 Reactor antineutrino flux and spectrum

With 621 days of data, the IBD yield was measured with the eight detectors at Daya Bay<sup>10</sup>. In addition, the ratio of measured to the predicted flux is found to be  $0.946 \pm 0.020$  for the Huber+Mueller model, which is consistent with the global average of previous short baseline experiments (Fig. 7). However, an older model based on the ILL measurements on reactor isotopes and a theoretical calculation of  $^{238}\text{U}$  by Vogel *et al.*, would lead to a ratio of  $0.992 \pm 0.021$ . We also observed a  $2.9\sigma$  deviation in the measured energy spectrum as compared to the predicted one. In particular, in the region of 4-6 MeV, a local significance of  $4.4\sigma$  was found with a clear excess (Fig. 8).

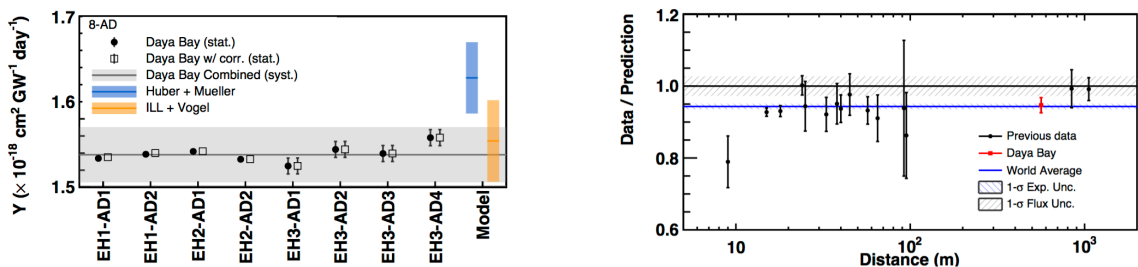


Figure 7 – Left: the IBD yield measured in eight detectors at Daya Bay. Right: the ratio of the measured to the predicted antineutrino flux at Daya Bay and the previous short baseline reactor experiments.

78

### 3.5 Fuel evolution analysis

With 1230 days of data, the evolution of IBD yield and energy spectrum has been confirmed by Daya Bay<sup>11</sup>. A change in the IBD yield per fission is observed to be  $d\sigma_f/dF_{239} = (-1.86 \pm 0.18) \times 10^{-43} \text{ cm}^2/\text{fission}$  over a range of the effective fission fraction of  $^{239}\text{Pu}$  from 0.25 to 0.34 (left panel of Fig. 9). The corresponding measurement of the IBD yield per fission was found to

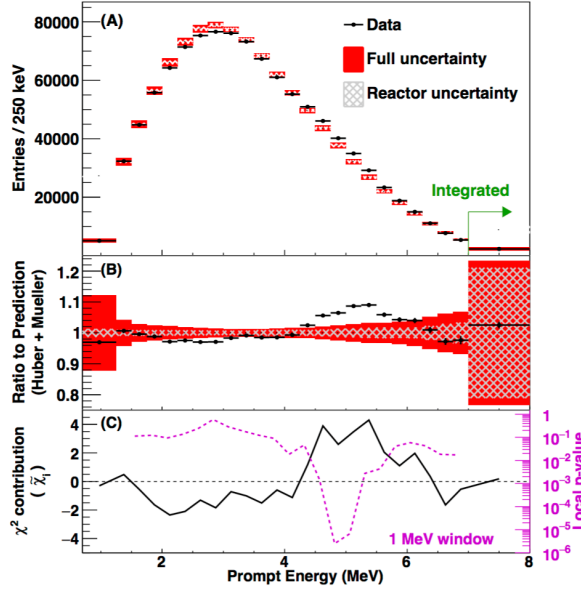


Figure 8 – The positron energy spectrum of the IBD candidates measured at Daya Bay. The spectrum shows an excess compared to the predicted one in the region [4,6] MeV.

84 be  $(6.17 \pm 0.17)$  and  $(4.27 \pm 0.26) \times 10^{-43} \text{ cm}^2/\text{fission}$  for the two dominant fission isotopes  $^{235}\text{U}$   
85 and  $^{239}\text{Pu}$ , respectively (right panel of Fig. 9). As compared to the Huber model, the bias in  
the prediction of the  $^{235}\text{U}$  flux becomes a possible explanation of the RAA.

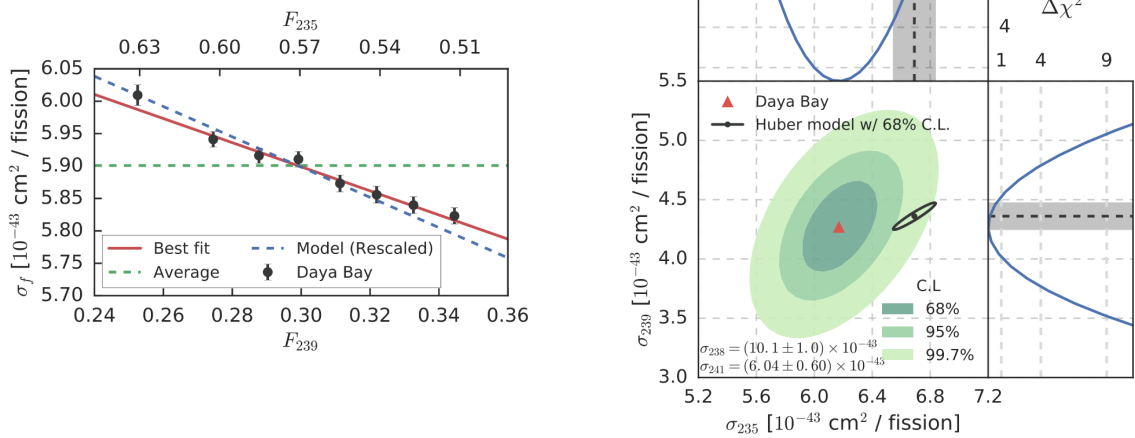


Figure 9 – Left: IBD yield per fission versus effective fission fraction of  $^{239}\text{Pu}$ , or  $^{235}\text{U}$ . Right: best-fit contour of the IBD yield per fission from  $^{239}\text{Pu}$  and  $^{235}\text{U}$ .

86

## 87 Acknowledgments

88 Daya Bay is supported in part by the Ministry of Science and Technology of China, the U.S.  
89 Department of Energy, the Chinese Academy of Sciences, the CAS Center for Excellence in  
90 Particle Physics, the National Natural Science Foundation of China, the Guangdong provincial  
91 government, the Shenzhen municipal government, the China General Nuclear Power Group, Key  
92 Laboratory of Particle and Radiation Imaging (Tsinghua University), the Ministry of Education,  
93 Key Laboratory of Particle Physics and Particle Irradiation (Shandong University), the  
94 Ministry of Education, Shanghai Laboratory for Particle Physics and Cosmology, the Research

95 Grants Council of the Hong Kong Special Administrative Region of China, the University De-  
96 velopment Fund of The University of Hong Kong, the MOE program for Research of Excellence  
97 at National Taiwan University, National Chiao-Tung University, and NSC fund support from  
98 Taiwan, the U.S. National Science Foundation, the Alfred P. Sloan Foundation, the Ministry of  
99 Education, Youth, and Sports of the Czech Republic, the Joint Institute of Nuclear Research in  
100 Dubna, Russia, the National Commission of Scientific and Technological Research of Chile, and  
101 the Tsinghua University Initiative Scientific Research Program. We acknowledge Yellow River  
102 Engineering Consulting Co., Ltd., and China Railway 15th Bureau Group Co., Ltd., for building  
103 the underground laboratory. We are grateful for the ongoing cooperation from the China General  
104 Nuclear Power Group and China Light and Power Company.

105 **References**

- 106 1. B. Pontecorvo, *Zh. Eksp. Teor. Fiz.* **33**(2), 549551 (1957)
- 107 2. Daya Bay Collaboration (F. P. An *et al.*), *Phys. Rev. Lett.* **108**, 171803 (2012)
- 108 3. Double Chooz Collaboration (Y. Abe *et al.*), *Phys. Rev. Lett.* **108**, 131801 (2012)
- 109 4. RENO Collaboration (J. K. Ahn *et al.*), *Phys. Rev. Lett.* **108**, 191802 (2012)
- 110 5. G. Mention *et al.*, *Phys. Rev. D* **83**, 073006 (2011)
- 111 6. Daya Bay Collaboration (F. P. An *et al.*), *Phys. Rev. D* **95**, 072006 (2017)
- 112 7. Daya Bay Collaboration (F. P. An *et al.*), *Phys. Rev. D* **93**, 072011 (2016)
- 113 8. Daya Bay Collaboration (F. P. An *et al.*), *Phys. Rev. Lett.* **117**, 151802 (2016)
- 114 9. Daya Bay Collaboration (F. P. An *et al.*), *Phys. Rev. Lett.* **117**, 151801 (2016)
- 115 10. Daya Bay Collaboration (F. P. An *et al.*), *Chinese Physics C* **41**(1), 13002-013002 (2017)
- 116 11. Daya Bay Collaboration (F. P. An *et al.*), *Phys. Rev. Lett.* **118**, 251801 (2017)